Hindawi
Bioinorganic Chemistry and Applications
Volume 2023, Article ID 7187387, 12 pages
https://doi.org/10.1155/2023/7187387

Research Article

Effect of Capping Agent on Structure, Composition, and Optical Properties of Low-Cost Chemically Deposited Zinc Oxide Thin Films and Their Antibacterial Activities

S. Thanikaikarasan,[1] **C. Amutha**,[2] **B. Natarajan**,[2] **D. Dhanasekaran**,[3] **and S. Rajkumar**[4]

[1]*Department of Physical Sciences, Saveetha School of Engineering, SIMATS, Chennai-602 105, Tamil Nadu, India*
[2]*Research Department of Physics, RDGA College, Sivagangai-630 561, Tamil Nadu, India*
[3]*Department of Electronic and Communication Engineering, Saveetha School of Engineering, SIMATS, Chennai-602 105, Tamil Nadu, India*
[4]*Department of Mechanical Engineering, Faculty of Manufacturing, Institute of Technology, Hawassa University, Awasa, Ethiopia*

Correspondence should be addressed to S. Rajkumar; ccetraj@gmail.com

Received 24 December 2022; Revised 16 April 2023; Accepted 7 October 2023; Published 23 October 2023

Academic Editor: Chun Xu

In the present report, pure zinc oxide and albumen-capped zinc oxide thin films were deposited on a glass substrate by a simple chemical method. The growth rate of the deposited film increases by means of number of dipping linearly. The films deposited were subjected to XRD, SEM, EDX, and UV-visible spectroscopy to analyze the crystal structure, morphology, composition, and optical properties. Structural feature reported that the deposited films were found to be a wurtzite structure. The degree of crystallinity depends on film thickness with deposition time per cycles. The parameters related to film structure, such as stress, strain, dislocation density, lattice constant, and bond length, were determined. The values of the fundamental absorption edge were at 3.28 and 3.06 eV for the deposited films of pure zinc oxide and albumen-capped zinc oxide, respectively. Photoluminescence measurements indicated that the peaks of emission were found to be 375 and 340 nm for zinc oxide and albumen-capped zinc oxide. The effects of an antibacterial activity against different positive and negative bacteria sources were determined.

1. Introduction

Transparent conducting oxides found extensive application in liquid crystal displays, transducers, and solar cells. The efficiency of the devices strongly depends upon materials, important key properties, high electrical conductivity with its transparency [1–3]. The materials such as cadmium oxide, indium oxide, and tin oxide plays a vital role in view of the fact that high transmission above wide spectral range have interesting characteristics such as moderately low cost and stability in the environment of chemistry [4–6]. Zinc oxide (ZnO) found to exist in wurtzite structure with band gap, binding energy values 3.3 eV, 60 meV attracted researchers to fabricate efficient optoelectronic devices [7, 8]. ZnO is predicted as an interesting candidate for devices such as gas sensors, solar cells, and photodiodes, and varistors and its different structure with physical, chemical, optical, and biological properties has attracted ZnO for medical and biological applications. ZnO thin films are mostly crystallized in wurtzite and cubic structures. Besides, it is a transparent material with different structures that could be synthesized in different forms of nanostructure [7, 8]. Several physical and chemical methods were employed for the preparation of ZnO thin films with cubic and hexagonal structures [9–14]. The method of SILAR is simply a two-step process for film preparation in which the substrate is immersed in

a precursor that consists of sources of cation with anion. The growth of the film deposition takes place consequently when it is dipped in precursors number of times [15]. The continuous reaction at optimized precursor concentration with solution pH values results on the formation of films on the substrate. The ZnO thin film was prepared by dipping the substrate in zinc acetate complex followed by dipping in a hot water bath at the boiling temperature of 95°C. Number of zinc complexes viz., sodium zincate, ammonium zincate prepared from zinc acetate, zinc sulphate, and zinc chloride were used as precursors for cation in film deposition by the SILAR method. The present work focused on the formation of ZnO thin films from ammonium zincate obtained from zinc chloride. The advantages and highlight of the technique is its simplicity of the equipment, ease to control the deposition rate with precursor concentration, and solution of pH values. SILAR is a simple wet chemical route for thin film synthesis in which the formation of film as a building block by ions instead of atoms, where the preparative parameters are controlled easily [16–19]. ZnO doped with individual elements such as Ag, Al, Bi, Cd, Co, Eu, and Mn which has been reported earlier [11, 12, 20–24]. By the comparison of a number of works for ZnO thin films with metallic dopants, few reports highlighted the growth and characterization of ZnO thin films mediated with bio-template such as silk [25], albumen [26], orange juice [26], and pea starch [27].

In the present report, ZnO and albumen-mediated (capped) ZnO thin films were deposited on a glass substrate made from zinc chloride, sodium hydroxide (NaOH), and liquid ammonia (NH_4OH) in addition with albumen as the capping agent by the simple SILAR method. The influence of the capping agent (albumen) on structure, composition, morphology, optical properties, FTIR, and photoluminescence measurement of the deposited films were reported. The effect of antibacterial activity against different bacteria sources was reported.

2. Experimental Details

The chemicals $ZnCl_2$, NaOH, liquid ammonia were purchased from Sigma Aldrich with 99.99% purity. The commercially purchased microscopic slides were cleaned using chromic acid followed by distilled water and ultrasonic cleaning with acetone and alcohol. The commercially purchased egg white layer (albumen) was used as a capping agent. The substrate was dipped in sodium zincite bath which was kept at temperature around 35°C for a well-known standardized time followed by the immersion process in boiled water for the same time of hydrogenation in which the water is maintained at temperature in the range between 90 and 95°C. Thin films of ZnO grown by the process of two-step chemical bath deposition method from a solution consist of 0.3 M $ZnCl_2$ and 0.3 M NaOH with a pH value maintained at 9.0 ± 0.1 and bath temperature 90°C under optimized condition. In the first dipping process, the ions in the solution get adsorbed over the substrate produced sodium zincite. Also, by following the same procedure with few number cycles by the incorporation of albumen as the capping agent with 0.3 M $ZnCl_2$ and 0.3 M NaOH. The prepared films were subjected to the process of annealing by keeping them in a muffle furnace at 300°C for 1 hour, thereafter taking them out to determine structure, morphology, composition, and optical properties. Figure 1 shows the experimental setup used for the preparation of pure and albumen-capped ZnO thin films. Structural feature of the prepared films was determined by an X-ray diffractometer (XPERTPRO PANalytical) with CuKα target radiation ($\lambda = 1.5406$ Å). Microscopic view with film composition was analyzed using a JEOL JSM 840 scanning electron microscope. The optical absorbance and transmittance of the deposited films was determined using a SHIMADZU 2000 ultra-violet-visible spectrophotometer. Photoluminescence measurement for the prepared samples was analyzed by PERKIN ELMER LS55 spectrofluorometer. Also, the appearance of bonds in the deposited films was determined using a SHIMADZU 8400S FTIR spectrometer. The effect of antibacterial activity for Gram (+) and Gram (−) sources was determined by disc diffusion method.

3. Results and Discussion

3.1. Film Thickness. The growth rate, deposition of ZnO, and albumen-capped ZnO on glass substrates were controlled by separate variables thickness and surface morphology [28–30]. The zinc chloride complex was prepared by dissolving 3.344 g $ZnCl_2$ in 250 cc demineralized water to attain a chemical solution of 0.3 M $ZnCl_2$. The solubility of zinc chloride is difficult leads to produce precipitation of the solution which is dissolved by the incorporation of few drops of acetic acid produces a transparent solution. The transparent solution has the solution pH value of 4.5 ± 0.1 as estimated by digital pH meter (HANNA instruments). The concentration of $ZnCl_2$ was found to be higher than 0.3 M in addition with 0.075 M NaOH, and particulate absorption takes place on the substrate surface that leads to produce films with poor quality. The molarity of $ZnCl_2$ was found to be 0.3 M $ZnCl_2$ and higher amount of 0.075 NaOH was added which leads to increase the pH value upto 9.0 ± 0.1, producing films with higher thickness and well-defined crystallinity. The higher value of NaOH with 0.3 M $ZnCl_2$ increases the pH value above 9.0 ± 0.1, and there is detachment of film from the substrate not from the layers on the substrate. The dependency of deposition time with films thickness and number of dipping for the deposited films on substrate is shown in Figure 2. Thickness of the deposited films was estimated by the measurement of weight difference for films deposited before and after certain intervals of time deposition on the substrate and the film thickness was determined using the following equation:

$$t = \frac{m}{A\rho}. \quad (1)$$

It is noted that the film thickness increases linearly with rate of 5 more dippings for both ZnO and albumen-capped ZnO. The observation reflects a small variability in the deposition process arising probably from small experimental scattered in deposition parameters bath concentration, temperature as well as due to the nonuniformity of film from

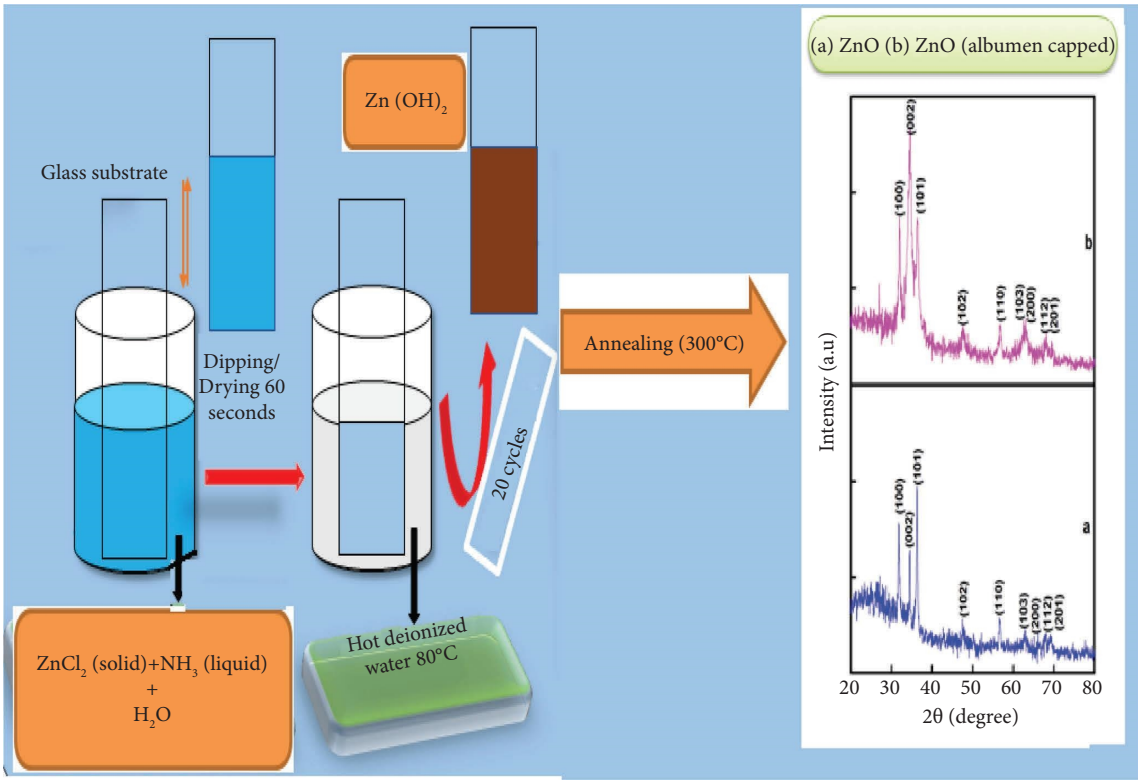

Figure 1: Experimental setup used for the preparation of ZnO and albumen-capped ZnO thin films.

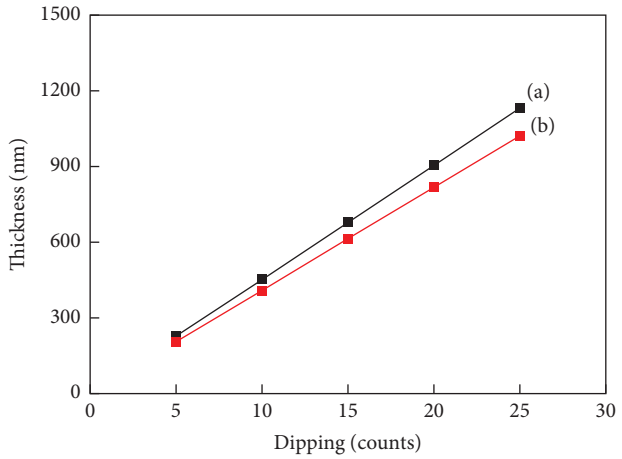

Figure 2: Variation of film thickness with number of dippings for (a) ZnO and (b) albumen-mediated ZnO thin films.

the substrate handling procedure as the deposition is carried out manually. The process has been carried out for ZnO and albumen-capped ZnO thin films.

3.2. Structural Properties. XRD pattern was obtained to identify the nature, structure, and phase of the deposited ZnO and albumen-capped ZnO thin films (Figure 3(a)). Several researchers reported that the ZnO thin films have cubic and hexagonal structures. Figure 3(a) revealed that the prepared films possess polycrystalline nature with a wurtzite structure. There are no additional secondary peaks in the XRD pattern, which denoted the films were devoid of impurities. The position of XRD pattern confirmed that the observation of diffraction angles at 36.32, 47.56, 56.52, 62.23, 66.42, 68.06, and 69.14 corresponds to the planes (100), (002), (101), (102), (110), (103), (200), (112), and (201) with prominent reflection along (101) for the films of pure ZnO with hexagonal crystal symmetry. The observed results were found to be in close agreement with standard file for hexagonal ZnO [30]. The peak intensity of (101) plane is found to be higher when compared with intensities of the all other planes, respectively. The diffraction pattern of albumen-capped ZnO thin films deposited on glass substrate is shown in Figure 3(b). It is evidenced that there is a slight shift in 2θ value when compared with results of pure ZnO. The intensity of (002) plane is maximized, which denoted the ZnO thin films with orientation along c axis when it is deposited additionally with albumen as the capping agent with pure ZnO. The observed characteristic results reported that any peaks corresponding to secondary elements as capping agent not present in EDX pattern as shown in Figure 3(b). There is observation of slight shift in 2θ value of ZnO thin films in addition with albumen as capping agent which produces films with slight difference in 2θ values as shown in Figure 3(b). The growth of ZnO thin films along c axis orientation is greatly favoured by the polar structure of ZnO, and it consists of Zn^{2+} and anion O^{2-} with its high polarity [31]. The observed peak intensity (002) along c axis is found to be a film with higher thickness value which has been measured using weight difference method. The intensity of (002) and (101) plane is found to be higher for films

have higher thickness around 1000 nm for ZnO, 960 for albumen-capped ZnO. As the time increases, the thickness of the deposited films tends to increase and thereafter decreases for higher deposition time, due to the overgrowth of the film [31]. The value of average crystallite size with grain sizes was obtained from X-ray line broadening analysis using the Scherrer equation assuming Gaussian-shaped peaks [15]. It is evident that the capping of albumen with ZnO produces variation of structural properties which are peaks of FWHM data, the peak position of diffraction angle 2θ, the crystallite size, lattice constant (c), the dislocation density (δ), and strain (ε) were determined. It is seen from the Table 1 that the lattice constant is found to increase by the addition of lesser amount of the capping agent. The crystallite size of the deposited films is calculated using the following equation: [32]:

$$D = \frac{0.9\lambda}{\beta \mathrm{COS}\theta}. \tag{2}$$

The value of force acting on the deposited films to restrict the formation of crystallites on the substrate is calculated using equation (3). Dislocation density and bond length for the ZnO and albumen-capped ZnO thin films were determined using the following equations [15, 29, 31, 33]:

$$\frac{1}{d^2} = \frac{4}{3}\left[\frac{h^2 + \mathrm{hk} + l^2}{a^2}\right] + \frac{l^2}{c^2}, \tag{3}$$

$$\beta = \left[\frac{\lambda}{D\cos\theta} - \varepsilon \tan\theta\right]. \tag{4}$$

The value lattice constants ("a" & "c"), unit cell volume, c/a ratio, atomic packing factor, and bond length were determined according to the following equations [28]:

$$v = \frac{\sqrt{3}}{2}a^2 c,$$

$$\mathrm{APF} = \frac{2\pi a}{3c\sqrt{3}}, \tag{5}$$

$$L = \sqrt{\left[\left(\frac{a^2}{3c^2}\right) + \left(\frac{1}{2} - u\right)^2 c^2\right]}.$$

The stress value present in ZnO and albumen-capped ZnO has been determined using the following equation:

$$\sigma = -233\frac{c - c_O}{c_O}, \tag{6}$$

$$\sigma = -233\,\frac{a - a_a}{a_0}. \tag{7}$$

The estimated value of lattice parameters for ZnO and albumen-capped ZnO thin films is given in Table 1.

3.3. Morphology and Film Composition. Morphological feature along with film composition for ZnO and albumen-capped ZnO was analyzed by EDX with SEM. The SEM image of ZnO and albumen-capped ZnO deposited on glass substrate is shown in Figure 4. It is found that albumen added as a capping agent there is no change in surface morphology for deposited films. A number of crystallites were grouped together to form a grain. The sizes of the grains were found to be between 0.7 and 0.9 μm. The average sizes of the grains were found to be 760 nm. Similar observation for albumen-mediated ZnO thin films reported earlier [34]. EDX spectra recorded for ZnO and albumen-capped ZnO thin films are denoted in Figures 5(a) and 5(b). The observation of emission lines Zn and O present in the investigated energy range indicated the formation of ZnO thin films as EDX spectra as in Figure 4(a). Similarly, the EDX spectra of albumen-capped ZnO thin films represent the Zn and O emission lines in the investigated energy range, but there are no impurities excluding albumen that can be acted as a capping agent in the deposited films. The capping agent added produces a slight change in stoichiometric ratio of Zn and O of the deposited films on the substrate (Figure 5(b)).

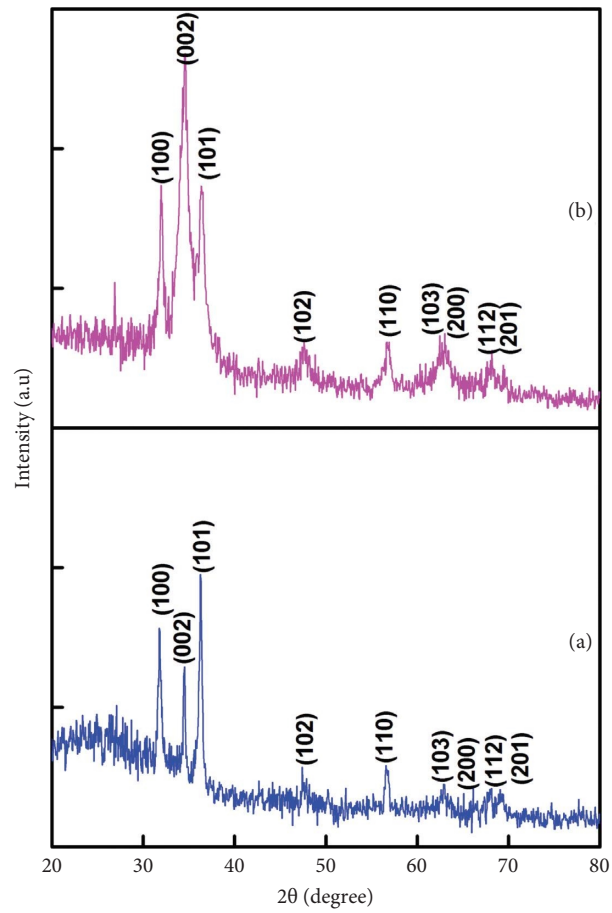

Figure 3: X-ray diffraction pattern of (a) ZnO and (b) albumen-mediated ZnO thin films.

3.4. Ultraviolet Visible Spectroscopy. The investigation of semiconductors by the route of optical absorption provides scientific explanation, concerning the band structure and the energy gap value of the deposited films. The percentage of absorption, transmittance for the deposited ZnO, and

Table 1: Structural parameters for SILAR-deposited ZnO and albumen-capped ZnO thin films.

Samples	Thickness (nm)	*Lattice constants (Å)*		*c/a*	Unit cell volume ($Å^3$)	APF	Bond length, *L* (Å)	Crystallite size, (D) (nm)	Strain, (ε) x 10^{-3}\ ($line^{-2}$ $metre^{-4}$)	Dislocation density, (δ) (10^{14} lines $metre^{-2}$)
		c	*a*							
ZnO	1130	5.105	3.004	1.699	39.89	0.702	1.220	35	1.019	8.163
Albumen-capped ZnO	1120	5.166	3.112	1.660	43.32	0.728	1.227	21	1.631	22.673

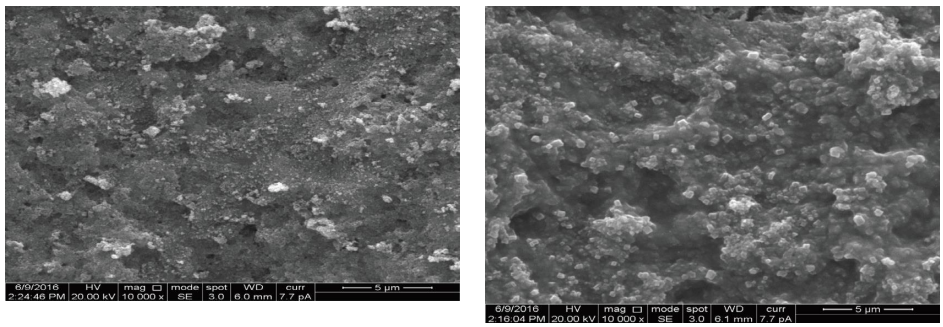

(a) (b)

Figure 4: Scanning electron microscope image of (a) ZnO and (b) albumen-mediated ZnO thin films.

albumen-capped ZnO films was estimated using a SHIMADZU spectrophotometer. The band gap value of the deposited films was determined using the following equation:

$$\alpha h\nu = A\left(h\nu - E_g\right)^n. \quad (8)$$

The absorbance spectra recorded for ZnO and albumen capped ZnO thin films are shown in Figure 6. It is noted that the deposited films had less absorption in the visible region. The behavior of absorption spectra which may be dependent upon film thickness deposited and also, there is a correlation between transmittance and absorbance of the deposited films. The band gap value of the deposited films was obtained by the extrapolation of linear portion of the energy axis at zero absorption coefficient (Figure 7). The band gap value was found to be 3.28 and 3.61 eV for ZnO and albumen-capped ZnO, respectively [34, 35]. There is a shift in the band gap value which can be due to the thickness value of the deposited films. Similar behavior was exhibited by albumen-capped ZnO films that were reported earlier [35].

3.5. FTIR Spectroscopy. FTIR spectroscopy is an important analytical tool to categorize the chemical bonds, composition, and element present in the deposited ZnO and albumen-capped ZnO thin films. The spectroscopic observation was carried out in between the wave number 400 and 4000 cm^{-1}. Figure 8 shows the FTIR spectra recorded for ZnO and albumen-capped ZnO thin films deposited on glass substrate. The peak appearance at 848 cm^{-1} responds to stretching mode of Zn-O bond present in the deposited films. The peak appeared at 1450 cm^{-1} which is responsible for asymmetric, symmetric stretching modes of C=O bonds in addition with associated with present in the deposited films after certain intervals of time as indicated in Figure 7(a) [36]. The FTIR spectra recorded for albumen-capped ZnO thin films deposited on glass substrate is shown in Figure 7(b). The observed peak intensity at 1585, 1018 cm^{-1} which may be attributed to C=C, Zn-O bands indicates capping effect of albumen with ZnO. The transformation of OH^- organic phase takes place due to the abovementioned process. The appearance of broad absorption peak at 3400 cm^{-1} is probably due to superimposition of N-H stretching of amide group at 3450 cm^{-1} by the bio-template and O-H stretching mode of water molecules. Besides, the appearance of some of the absorption bands in the range between 1316 and 1585 cm^{-1} may be due to C=O and C=C stretching modes of albumen as well as the new peak observed at 2900 cm^{-1} due to symmetric and asymmetric C-H bonds, respectively. The observed results are in close agreement with the results reported earlier [37]. The observed bands at 1557 and 3452 cm^{-1} may be due to stretching frequency of OH group absorbed at ambient atmosphere [38].

3.6. Photoluminescence. Photoluminescence measurements were taken out to identify the observation of peak shift emission for films of ZnO and albumen capped ZnO. The photoluminescence spectra of for ZnO and albumen-capped ZnO thin films obtained by the SILAR technique are shown in Figure 8. It is noted that there is strong that peak emission at 440 nm corresponding to blue emission has been observed due to the process of surface defect in ZnO mainly due to Zn vacancy and weak green emission band approximately at 500 nm known as a deep level

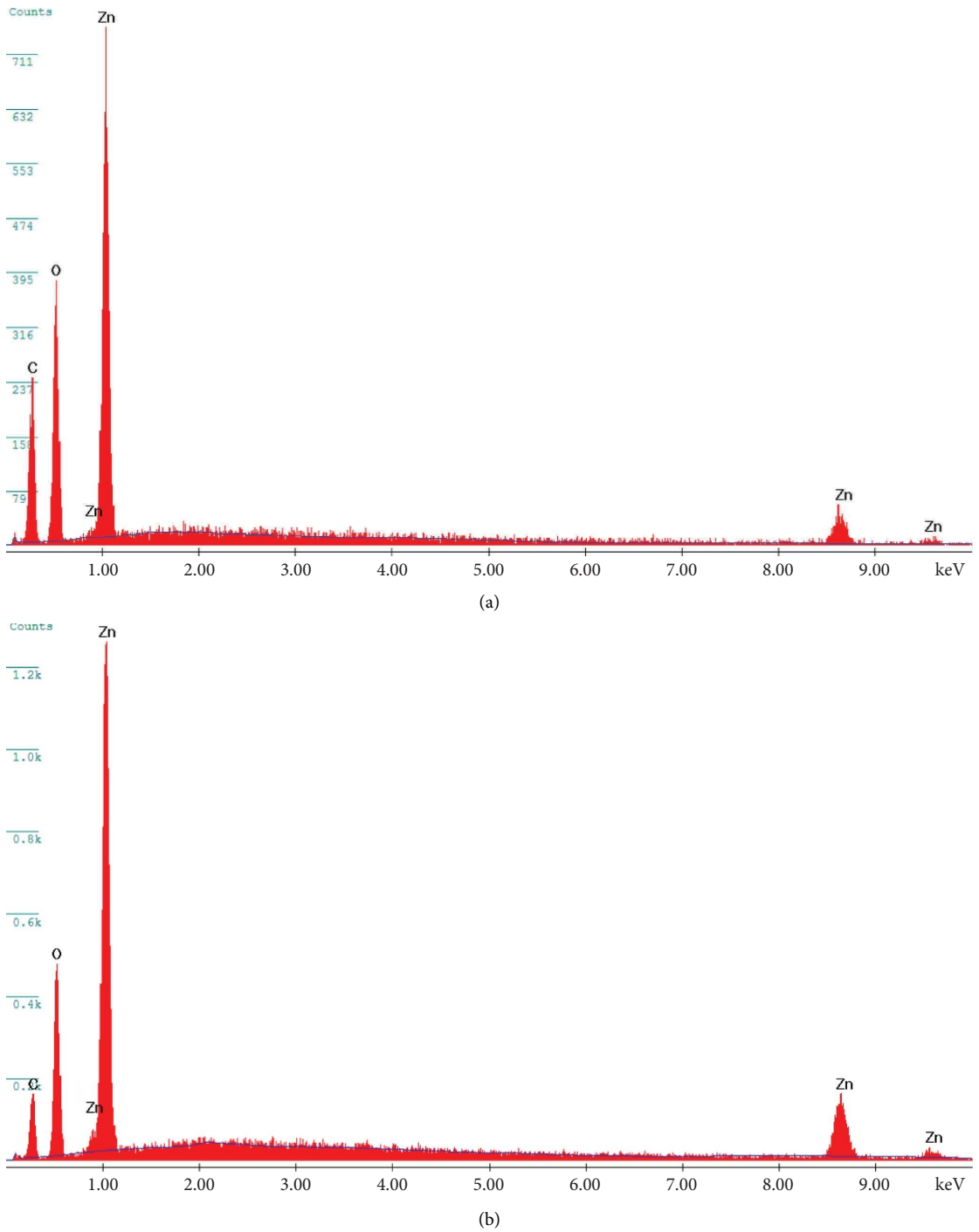

Figure 5: EDX pattern of (a) ZnO and (b) albumen-capped ZnO SILAR deposited thin films.

emission related to the states of defect in the deep level [16]. The oxygen vacancy present in single ionized level which is responsible for this green emission in the ZnO [17]. It may result from the process of recombination of photo-generated hole with an electron occupying the oxygen vacancies with interstitials of zinc. The albumen capped ZnO thin films denoted peak emission at wavelength 380 nm, and they also have a weak blue emission peak located at 420 nm (Figure 8(b)). The ultraviolet emission is known as a near-band emission, originating from the recombination of free exciton through an exciton-exciton collision process [18]. In all the samples, the emission of ultraviolet was found to be most prominent. But the albumen capped with ZnO thin films sample a dramatic change in emission spectrum was observed. The observation of ultraviolet emission peaks at 440–500 nm (Z_3g and Z_6g) (with the blue shift of single emission peak), which is considered as a signature of charge transfer reaction [19].

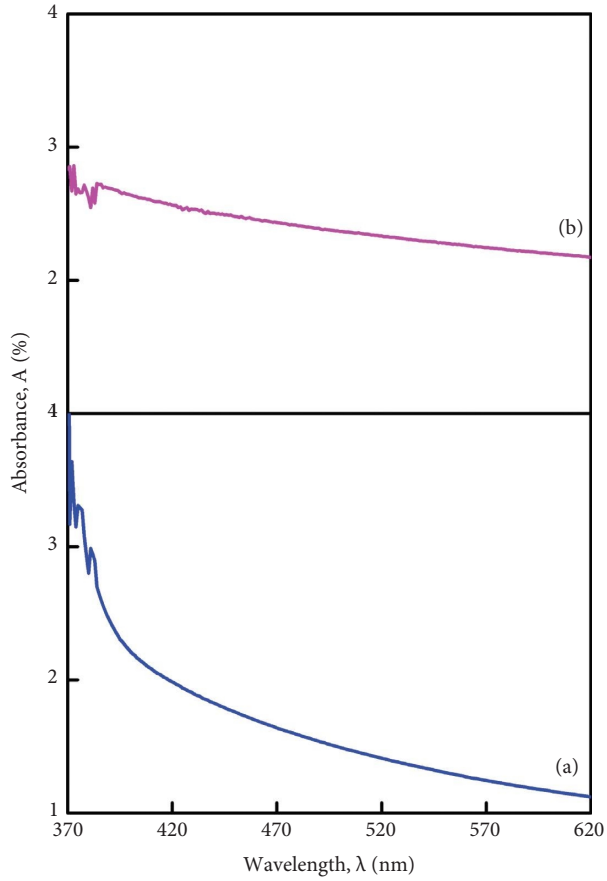

Figure 6: Optical absorption spectra of (a) ZnO and (b) albumen-mediated ZnO thin films.

3.7. Antibacterial Activity. The efficiency of antibacterial activity for ZnO and albumen-capped ZnO thin films were tested by disc diffusion method. The samples such as ZnO and albumen-capped ZnO deposited on glass substrate were taken out from the substrate by the process of scratching method and the powder sample with diameter of zone of inhibition around the membranes after 24 hours were measure as 12, 10, 5, 3, 5, and 14 mm for *Escherichia coli*, *Pseudomonas aeroginosa*, *Streptococcus agalactiae, Staphylococcus auereus, Salmonella typhimurium, and Klebsiella pneumonia*, respectively. Pure ZnO and capped ZnO powder taken out from the substrate and the sample diameters of the zone of inhibition around the membranes after 24 hours were measured as 12, 10, 5, 3, 5, and 14 mm for *E coli, Paerogi-nosa, Sagalactiae, Staphylococcus auereus, Salmonella typhimurium, and Klebsiella pneumonia*, respectively. After 48 hours of incubation, the diameter of the zone of inhibition was found to increase as shown in Figure 9. Pure ZnO have low antibacterial activity against E. coli was investigated. The albumen capped ZnO sample diameters of the zone of inhibition around the membrane after 24 hours were measured at 18, 9, 12, 5, and 8 mm for E. coli, P. aeroginosa, S. agalactiae, S. auereus, S. typhimurium, and K. pneumonia, respectively. The zone inhibition diameter of samples found to increase after 48 hours which is shown in Figure 10. As a result, the samples influence strong influence against sources such as E. coli than S.auereus, and such observation found to close agreement with value reported earlier [25–27, 39]. The cell nature with structure is one the favourable reason for difference in sensitivity. The formation zone of inhibition has clearly indicated the antibacterial activity against ZnO nanostructure. The value of zone inhibition of different bacteria sources for ZnO and albumen capped ZnO thin films at 24 and 48 hours is given in Table 2. We have concluded that albumen capped ZnO found to exhibit higher value antibacterial activity for *E. coli* and *S. auereus* bacterial than ZnO (see Figure 11).

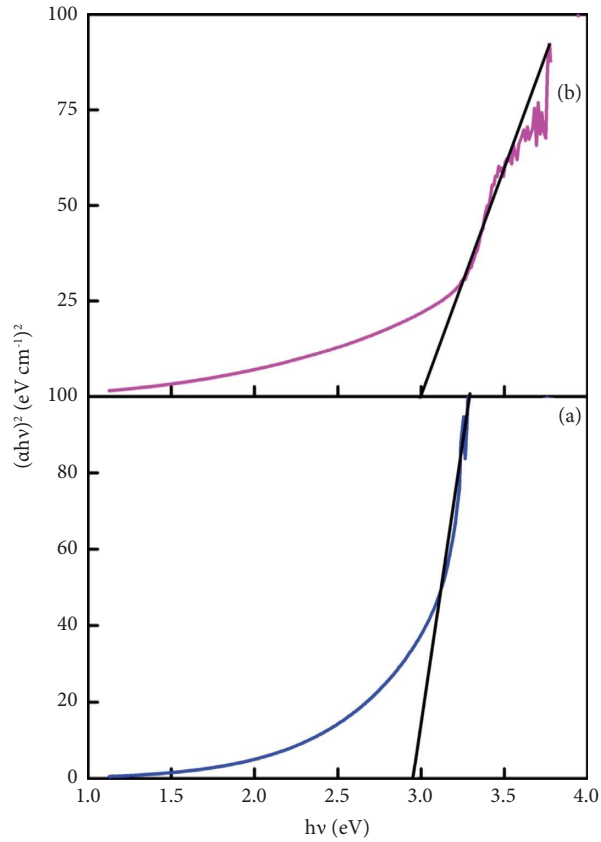

Figure 7: Plot of $(h\nu)$ versus $(\alpha h\nu)^2$ for (a) ZnO and (b) albumen-mediated ZnO thin films.

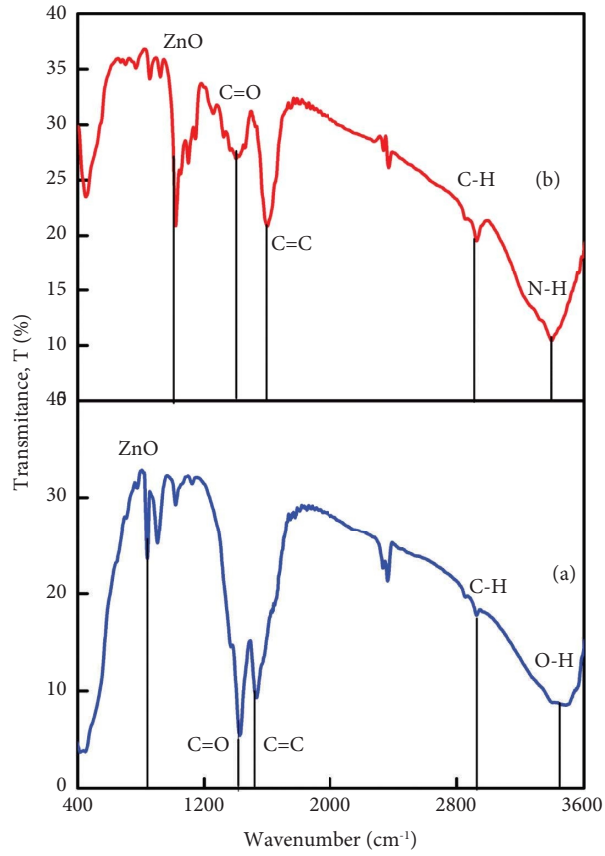

Figure 8: FTIR spectra of (a) ZnO (b) albumen-mediated ZnO thin films.

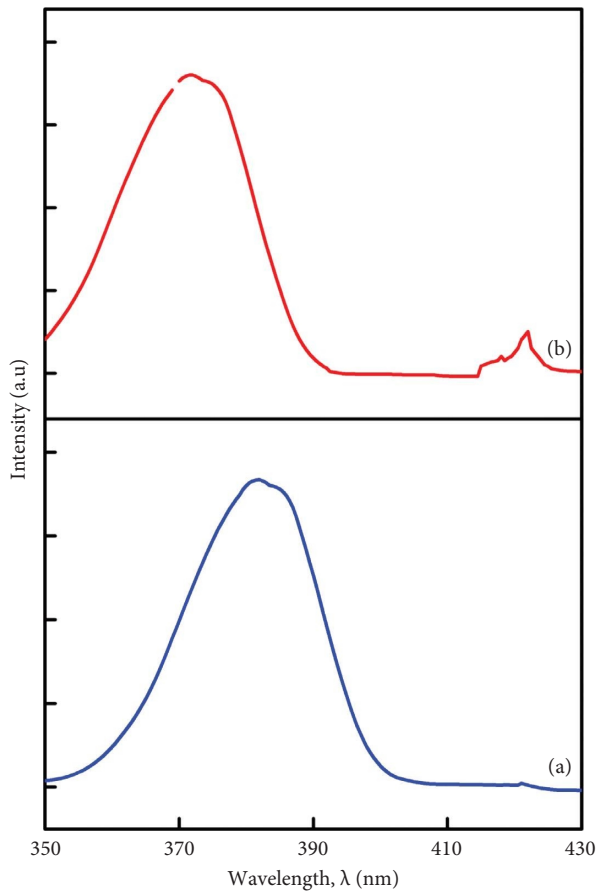

Figure 9: Photoluminescence spectra of (a) ZnO and (b) albumen-mediated ZnO thin films.

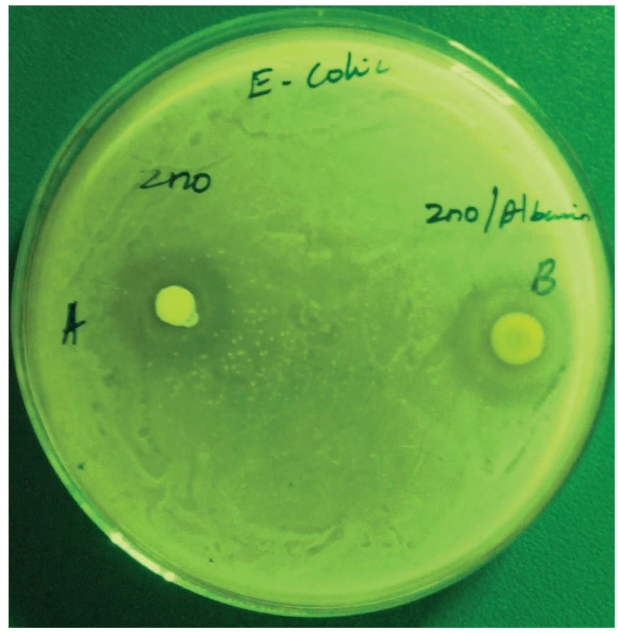

Figure 10: Antibacterial activity analysis results on *E coli* bacteria for pure ZnO, albumen-mediated ZnO thin films at time period of incubation at 24 hour.

Table 2: Zone of inhibition of different bacteria sources for ZnO and albumen-capped ZnO thin films at 24 and 48 hours.

S.No	Bacteria	*Zone of inhibition in diameter (mm)*			
		ZnO		*Albumen-capped ZnO*	
		24 hrs	48 hrs	24 hrs	48 hrs
1	*Escherichia coli*	17	18	21	22
2	*Staphylococcus aureus*	15	18	21	22

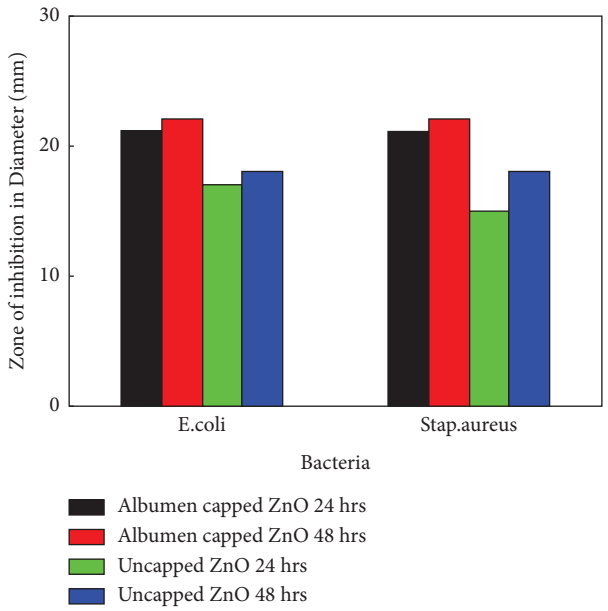

Figure 11: Zone of inhibition on bacterial species for ZnO and albumen-capped ZnO thin films.

4. Conclusions

The aim of this research report was to explain the effect of albumen as capping agent with ZnO thin films prepared by the simple SILAR method. Structural properties reported that the prepared films exhibited hexagonal structure with orientation along (101) and (002) for ZnO and albumen capped ZnO. Microscopic observation reported that the films have grain such as structure with low density. EDX analysis reported that the replacement of capping agent in addition with the presence of elements as stoichiometry (Zn:O) in the deposited films. The shift in energy gap was determined as 3.28, 3.61 eV for the deposited ZnO and albumen-capped ZnO with different film thickness values. FTIR results indicated that the appearance stretching mode at 848 cm^{-1}, 1018, cm^{-1} corresponding to Zn-O, whereas the band in present at 1585 cm^{-1} corresponding C=C response to effect of capping agent albumen with ZnO. The appearance of band absorbance in between 1316 and 1585 cm^{-1} corresponding stretching modes of albumen also the new observed peak at 2900 cm^{-1} corresponding to symmetric, asymmetric modes of C–H, respectively. The broad absorption peak at 3400 and 1325 cm^{-1} is probably due to superimposition of N-H stretching of amide group with water molecules. Photoluminescence measurements reported that the peaks of emission of ultraviolet blue are at 375 and 340 nm, respectively. The films of ZnO capping with albumen were found to possess higher value of activity than ZnO corresponding to change in surface morphology with increase in surface of the deposited films. Due to the reason of nontoxicity and intense antibacterial activity with some other noble properties of ZnO, capping ZnO with albumen found to exhibit antibacterial activity effect against bacteria sources in nanotechnology. [40, 41].

Data Availability

The data used to support the findings of this study are included in the paper. Further information or data are available from the corresponding author upon request.

Conflicts of Interest

The authors declare that there are no conflicts of interest regarding the publication of this paper.

Acknowledgments

The authors acknowledge the Saveetha School of Engineering, Saveetha Institute of Medical and Technical Sciences, provided to carry out this kind of research work and publication in the journal. The authors thank Management of Saveetha School of Engineering, Saveetha Institute of Medical And Technical Sciences, India, for their appreciation and encouragement to complete this research work with in-house research facilities.

References

[1] X. Han, R. Liu, and Z. Xu, "Structural and optical properties of rock-salt Cd1−xZnxO thin films prepared by thermal decomposition of electrodeposited Cd1−xZnxO2," *Thin Solid Films*, vol. 517, pp. 5653–5657, 2009.

[2] R. Sarath babu, Y. Narasimha murthy, S. Vinoth et al., "Enhancement in optoelectronic properties of lanthanum co-doped CdO: Zn thin films for TCO applications," *Superlattices and Microstructures*, vol. 162, Article ID 107097, 2022.

[3] R. K. Gupta, K. Ghosh, R. Patel, S. R. Mishra, and P. K. Kahol, "Structural, optical and electrical properties of in doped CdO thin films for optoelectronic applications," *Materials Letters*, vol. 62, no. 19, pp. 3373–3375, 2008.

[4] S. G. Ruvalcaba-Manzo, S. J. Castillo, M. Flores-Acosta, R. Ochoa-Landín, and R. Ramírez-Bon, "Study of optical, morphological, structural, and chemical properties of CdO thin films synthesized by thermal annealing transformation of CdCO3 thin films," *Optical Materials*, vol. 132, Article ID 112742, 2022.

[5] M. Souli, L. Ajili, and N. K. Turki, "Enhancement in structural, optical and morphological properties of sprayed In2O3 thin

films induced by low energy electron beam irradiation," *Sensors and Actuators B: Chemical*, vol. 239, pp. 1185–1193, 2017.

[6] D. Kürschner, G. Hallum, S. Vogel, H. P. Huber, and W. Schulz, "Static and transient optical properties of thin film indium tin oxide during during laser excitation," *International Journal of Heat and Mass Transfer*, vol. 209, Article ID 124119, 2023.

[7] V. L. Patil, S. A. Vanalakar, P. S. Patil, and J. H. Kim, "Fabrication of nanostructured ZnO thin films based NO2 gas sensor via SILAR technique," *Sensors and Actuators B: Chemical*, vol. 239, pp. 1185–1193, 2017.

[8] S. Soepriyanto, A. A. Korda, and S. A. Dwiwanto, "Effect of ZnO nanoparticles to mechanical properties of thixoformed Mg-Al-Zn alloy," *Mater. Research and Exploration*, vol. 5, Article ID 036517, 2018.

[9] Y. R. Ryu, S. Zhu, J. D. Budai, H. R. Chandrasekhar, P. F. Miceli, and H. W. White, "Optical and structural properties of ZnO films deposited on GaAs by pulsed laser deposition," *Journal of Applied Physics*, vol. 88, no. 1, pp. 201–204, 2000.

[10] T. Ohgaki, N. Ohashi, H. Kakemoto et al., "Growth condition dependence of morphology and electric properties of ZnO films on sapphire substrates prepared by molecular beam epitaxy," *Journal of Applied Physics*, vol. 93, no. 4, pp. 1961–1965, 2003.

[11] M. Tamseel, K. Mahmood, A. Ali, K. Javaid, and H. Mufti, "Controlled growth of Ag-ZnO thin films by thermal evaporation technique for optimized thermoelectric power generation," *Journal of Alloys and Compounds*, vol. 938, Article ID 168507, 2023.

[12] N. H. Sheeba, S. C. Vattappalam, G. S. Okram et al., "Studies on Photoresponse and LPG sensitivity of transparent Al doped ZnO thin films prepared by thermal evaporation technique," *Mater. Research bulletin*, vol. 93, pp. 130–137, 2017.

[13] T. Tamseel, B. K. Mahmood, A. Ali, K. Javaid, and Hareem Mufti, "Controlled growth of Ag-ZnO thin films by thermal evaporation technique for optimized thermoelectric power generation," *Journal of Alloys and Compounds*, vol. 938, Article ID 168507, 2023.

[14] P. Rajkumar and B. K. Sarma, "Substrate dependent structural variations of biomimetic carbonated hydroxyapatite deposited on glass," *Ti and sputtered ZnO thin films*, vol. 191, Article ID 112120, 2022.

[15] P. Mitra and S. Mondal, "Structural and morphological characterization of ZnO thin films synthesized by SILAR," *Progress of Theoretical and Experimental Physics*, vol. 1, pp. 17–31, 2013.

[16] F. Mikailzade, H. Türkan, F. Önal, M. Zarbali, A. Göktaş, and A. Tumbul, "Structural and magnetic properties of polycrystalline Zn1−xMnxO films synthesized on glass and p-type Si substrates using Sol–Gel technique," *Applied Physics A*, vol. 127, 2021.

[17] P. Sreedev, V. Rakhesh, N. S. Roshima, and B. Shankar, "Preparation of zinc oxide thin films by SILAR method and its optical analysis," *Journal of Physics: Conference Series*, vol. 1172, Article ID 012024, 2019.

[18] S. K. Shaikh, S. I. Inamdar, V. V. Ganbavle, and Y. R. Kesu, "Chemical bath deposited ZnO thin film based UV photoconductive detector," *Journal of Alloys and Compounds*, vol. 664, pp. 242–249, 2016.

[19] I. Barceló, T. L. Villarreal, and R. Gómez, "Efficient sensitization of ZnO nanoporous films with CdSe QDs grown by successive ionic layer adsorption and reaction (SILAR)," *Journal Photochem. Photobio A Chem*, vol. 220, pp. 47–53, 2011.

[20] F. C. Correia, J. M. Ribeiro, A. Ferreira et al., "The effect of Bi doping on the thermal conductivity of ZnO and ZnO:Al thin films," *Vacuum*, vol. 207, Article ID 111572, 2023.

[21] S. Sharma, M. Tomar, V. Gupta, and A. Kapoor, "Investigation of cadmium-incorporated ZnO thin films for photodetector applications," *Superlattices and Microstructures*, vol. 151, Article ID 106812, 2021.

[22] A. Hassan, G. Li, S. Belakry et al., "Structural, morphological and transport properties of Ni doped ZnO thin films deposited by thermal co-evaporation method," *Materials Science in Semiconductor Processing*, vol. 123, Article ID 105530, 2021.

[23] S. Mondal, "Durga Basak "Photophysical investigation of the formation of defect levels in P doped ZnO thin films," *Ceream, Inter*, vol. 48, pp. 20000–20009, 2022.

[24] S. Mondal, S. R. Bhattacharyya, and P. Mitra, "Preparation of manganese-doped ZnO thin films and their characterization," *Bulletin of Materials Science*, vol. 36, pp. 223–229, 2013.

[25] J. Han, H. Su, J. Xu et al., "Silk mediated synthesis and modification of photoluminescent ZnO nanoparticles," *Journal of Nanoparticle Research*, vol. 14, p. 726, 2012.

[26] A. K. Jha, V. Kumar, and K. Prasad, "Biosynthesis of metal and oxide nanoparticles using orange juice," *Journal of Bionanoscience*, vol. 5, pp. 162–166, 2011.

[27] J. Yu, J. Yang, B. Liu, and X. Ma, "Preparation and characterization of glycerolplasticized-pea starch/ZnO-carboxymethylcellulose sodium nanocomposites," *Bio-Magnetic Research and Technology*, vol. 100, pp. 2832–2841, 2009.

[28] S. Thanikaikarasan, "Role of electrolyte concentration on growth kinetics, film thickness, structural, compositional and optical properties of cadmoselite thin films through electrochemical route," *Journal of Alloys and Compounds*, vol. 885, Article ID 160963, 2021.

[29] S. Thanikaikarasan, R. Perumal, and S. Roji Marjorie, "Influence of potential on structural, compositional, optical and magnetic properties of electrochemically grown iron selenide thin films," *Journal of Alloys and Compounds*, vol. 848, Article ID 156348, 2020.

[30] Pennsylvenia, *Joined Council for Powder Diffracted System International Centre for Diffraction Data, File No.36-1451*, Pennsylvenia, Pennsylvenia, PS USA, 2003.

[31] S. Mondal and P. Mitra, "Effect of manganese incorporation in ZnO thin films prepared by SILAR," *Science & Society*, vol. 10, p. 139, 2012.

[32] B. D. Cullity Bd and S. R. Stock, *Elements of X-ray Diffraction"*, Pearson Publishers, London, UK, 3rd edition, 2001.

[33] M. Voigt, M. Klaumünzer, H. Thiem, and W. Peukert, "Detailed analysis of the growth kinetics of ZnO nanorods in methanol," *Journal of Physical Chemistry C*, vol. 114, p. 6243, 2010.

[34] D. Jesuvathy Sornalatha, S. Bhuvaneswari, S. Murugesan, and P. Murugakoothan, "Solochemical synthesis and characterization of ZnO nanostructures with different morphologies and their antibacterial activity," *Optik*, vol. 26, no. 1, pp. 63–67, 2015.

[35] M. Shoeb, B. R. Singh, J. A. Khan, and W. Khan, "ROS-dependent anticandidal activity of zinc oxide nanoparticles synthesized by using egg albumen as a biotemplate," *Advanced. Nature and Science: Nanoscience and Nanotechnology*, vol. 4, pp. 035015–035026, 2013.

[36] X. Chu and H. Zhang, *Modern Applied Science*, vol. 3, pp. 177–181, 2009.
[37] X. T. Zhang, Y. C. Liu, J. Y. Zhang et al., "Structure and photoluminescence of Mn-passivated nanocrystalline ZnO thin films," *Journal of Crystal Growth*, vol. 254, no. 1-2, pp. 80–85, 2003.
[38] P. Jiang, J. Zhou, H. Fang, C. Wang, Z. L. Wang, and S. Xie, "Hierarchical shelled ZnO structures made of bunched nanowire arrays," *Advanced Functional Materials*, vol. 17, pp. 1303–1310, 2007.
[39] F. Nouroozi and F. Farzaneh, "Synthesis and characterization of brush-like ZnO nanorods using albumen as biotemplate," *Journal of the Brazilian Chemical Society*, vol. 22, pp. 484–488, 2011.
[40] A. J. C. Fiddes, K. Durose, A. W. Brinkman, J. Woods, P. D. Coates, and A. J. Banister, "Preparation of ZnO films by spray pyrolysis," *Journal of Crystal Growth*, vol. 159, no. 1-4, pp. 210–213, 1996.
[41] M. J. Alam and D. C. Cameron, "Preparation and properties of transparent conductive aluminum-doped zinc oxide thin films by sol–gel process," *Journal of Vacuum Science & Technology A*, vol. 19, no. 4, pp. 1642–1646, 2001.